

Lightcone renormalization and quantum quenches in one-dimensional Hubbard models

Tilman Enss¹ and Jesko Sirker²

¹*Physik Department, Technische Universität München, D-85747 Garching, Germany*

²*Department of Physics and Research Center OPTIMAS,
Technical University Kaiserslautern, D-67663 Kaiserslautern, Germany*

(Dated: September 8, 2022)

It follows from the Lieb-Robinson bound that the local Hamiltonian time evolution of an operator can be restricted to an effective light cone. Here we present a very efficient renormalization group algorithm based on this light cone structure to study the time evolution of prepared initial states in one-dimensional quantum systems. We use the algorithm to investigate the relaxation dynamics and possible thermalization of double occupancies in fermionic Hubbard models. For the integrable Hubbard model we find indications of a pure power-law decay while the decay becomes exponential when adding a nearest neighbor interaction. A description of the long-time behavior by thermal expectation values is possible but requires the use of negative temperatures.

PACS numbers: 02.70.-c, 05.70.Ln, 37.10.Jk, 71.27.+a

Using ultracold atomic gases as quantum simulators it has become possible to prepare states in almost perfectly isolated many-body systems and to monitor their time evolution [1, 2]. At the same time, enormous progress in numerical renormalization group methods has given us access to the dynamics in quantum models in one dimension (1D) [3–6]. Fundamental questions about the relaxation dynamics and the applicability of the eigenstate thermalization hypothesis (ETH) can therefore now be addressed both experimentally and numerically [1, 7, 8].

In this letter we present an algorithm to study the unitary time evolution of an initial state (IS) in a 1D quantum system. We concentrate here on the case of a product IS particularly relevant for experiment but note that the algorithm can also be generalized to a thermal IS. According to the Lieb-Robinson bound and recent generalizations [9], time evolution with a local Hamiltonian in a non-relativistic quantum theory gives rise to an effective light cone. Up to exponential tails, correlations and entanglement in such a system only spread with a finite velocity. We show that a Trotter-Suzuki decomposition (TSD) of unitary time evolution immediately leads to a light cone and that this light cone can be approximated in a truncated Hilbert space using density matrix renormalization group (DMRG) techniques [4, 10–13]. Contrary to time-dependent DMRG [3] an explicit calculation of eigenvectors of the system, which is the computationally most costly step, is not necessary. This makes the new light cone renormalization group (LCRG) algorithm extremely fast and efficient. Furthermore, the implementation of local conservation laws—important for an effective numerical study—becomes particularly simple. If the “speed of light” set by the TSD is larger than the Lieb-Robinson speed at which information spreads, then the algorithm directly yields results for the thermodynamic limit. Contrary to the infinite size time evolving block decimation (iTEBD) [6], however, it does not rely on translational invariance. In the second part of this let-

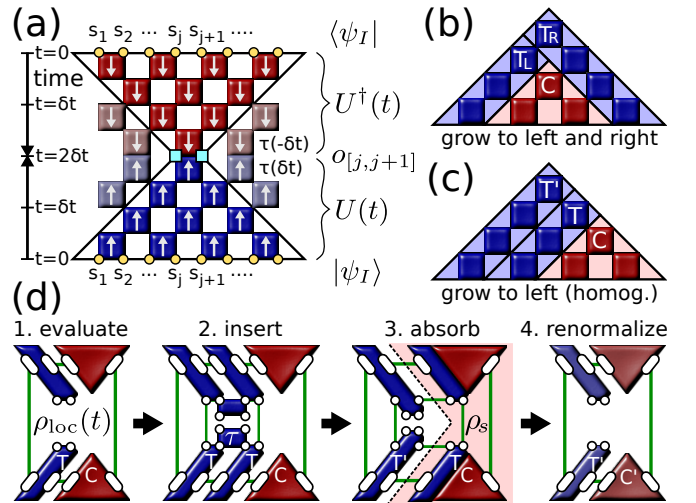


FIG. 1: (Color online) LCRG algorithm. (a) TSD of time evolution reveals light cone structure. (b) Lower light cone C grows alternately to upper left and right (general algorithm). (c) For homogeneous systems growth to upper left is sufficient. (d) Growth in four steps: 1. evaluate observable using local density matrix; 2. insertion of additional transfer matrix T and local update τ ; 3. absorption into larger C' , T' ; 4. renormalization to new block index.

ter we will apply the LCRG algorithm to the 1D version of a problem which has already been intensively studied in 3D [2, 14]: the relaxation of double occupancies in fermionic Hubbard models. We will investigate the differences between the integrable and non-integrable cases as well as a possible thermalization in the long-time limit.

The LCRG algorithm to calculate the time evolution

$$\langle o_{[j,j+n]} \rangle^I(t) \equiv \langle \Psi_I | e^{iHt} o_{[j,j+n]} e^{-iHt} | \Psi_I \rangle \quad (1)$$

of an observable $o_{[j,j+n]}$ acting on sites $j, j+1, \dots, j+n$ is based on corner transfer matrices [15] and inspired by

DMRG studies of dynamics in stochastic systems [11]. Here $|\Psi_T\rangle = |s_1 s_2 \dots\rangle$ is a product IS with s_j denoting states in the local basis and $H = \sum_j h_{j,j+1}$ is a Hamiltonian with nearest neighbor interaction. A TSD of the unitary time evolution operator then leads to the 2D lattice shown graphically in Fig. 1(a). It consists of local updates forward in time $\tau_{j,j+1}(\delta t) = \exp(-ih_{j,j+1}\delta t)$ ("↑" plaquettes) and backward $\tau_{j,j+1}(-\delta t) \equiv \tau_{j,j+1}^\dagger(\delta t)$ ("↓" plaquettes). Unless there is an operator insertion, facing plaquettes trivialize $\tau_{j,j+1}(-\delta t)\tau_{j,j+1}(\delta t) = \mathbb{1}$ (shaded plaquettes). This yields the light cone structure emanating from the local observable $o_{[j,j+n]}$ at time t . Instead of the first order TSD shown in Fig. 1 also higher order decompositions can be easily implemented. Neither translational invariance of the IS nor of the Hamiltonian are explicitly required for the general algorithm, cf. Fig. 1(b).

For a homogeneous system with a product IS of period one or two, it is sufficient to grow the light cone only to the left and forward in time, cf. Fig. 1(c). Growth proceeds in four steps shown in Fig. 1(d): 1. In the forward time evolution starting from the IS, a light cone C with left and right block indices of dimension χ (elliptic connectors) is joined with a left transfer matrix T which has two block indices and two single-site indices of dimension M (small circular connectors). The lower edges are contracted with the IS. The backward time evolution in the upper part of the figure is simply the adjoint of the forward evolution [20]. The resulting expression with four free site indices in the middle at time t is the local density matrix $\rho_{\text{loc}}(t)$ on two neighboring sites $j, j+1$ in the example shown in Fig. 1(a) and on sites $[j, j+n]$ in the general case. An expectation value is obtained as $\langle o_{[j,j+n]} \rangle^I(t) = \text{Tr}_{[j,j+n]}(\rho_{\text{loc}}(t) o_{[j,j+n]})$. 2. (Insertion) An additional transfer matrix T and local plaquette τ are inserted both in the forward and backward time evolution, and the previous free site indices are traced over. 3. (Absorption) T is joined with C to form a larger C' which will become the new C for the next time step. Similarly τ joins T to form the new T' . The reduced density matrix ρ_s is formed by tracing over the right block (χ) and site (M) indices of the light cone, $\text{Tr}_{\text{r.h.s.}}(TC)^\dagger(TC)$, but leaving open the left block and site indices [dashed line in Fig. 1(d)]. 4. (Renormalization) The old block index of C , T is combined with the additional single-site index into a new block index. The largest χ eigenvectors of ρ_s form the new reduced block basis.

Note that only summations and multiplications are required to build the light cone. Eigenvectors of the transfer matrix are automatically formed, which saves the most time-consuming step in standard transfer matrix DMRG algorithms. Only the density matrix ρ_s has to be diagonalized, which dominates the computation time $\sim \mathcal{O}(M^3\chi^3)$. Our algorithm therefore combines the speed of iTEBD with the flexibility of TEBD [5] to treat non-translationally invariant systems. Due to the local structure of the updates, conservation laws are easily im-

plemented in our algorithm (see below).

We use the LCRG algorithm with a second order TSD to study dynamics in the 1D fermionic Hubbard model

$$H_U = -J \sum_{j,\sigma=\uparrow,\downarrow} (c_{j,\sigma}^\dagger c_{j+1,\sigma} + h.c.) + U \sum_j n_{j\uparrow} n_{j\downarrow} \quad (2)$$

where J is the hopping amplitude, U the potential, and $n_{j,\sigma} = c_{j,\sigma}^\dagger c_{j,\sigma}$. As IS's we will consider the state where doubly occupied and empty sites alternate, $|\Psi_D\rangle = \prod_j c_{2j\uparrow}^\dagger c_{2j\downarrow}^\dagger |0\rangle$, and the Néel state, $|\Psi_N\rangle = \prod_j c_{2j+1\uparrow}^\dagger c_{2j\downarrow}^\dagger |0\rangle$. For these states, we want to investigate the time dependence of double occupancies, $d_j = n_{j\uparrow} n_{j\downarrow}$, and of the staggered magnetization, $m_j = (-1)^j S_j^z = (-1)^j (n_{j\uparrow} - n_{j\downarrow})/2$. The following symmetries of the Hubbard model allow us to establish various relations between the states and operators: (a) There is a unitary duality transformation $\mathcal{U} = \prod_j (c_{j\uparrow} + (-1)^j c_{j\uparrow}^\dagger)$ relating the repulsive ($U > 0$) and the attractive ($U < 0$) Hubbard models. This transformation leads to $\mathcal{U}^\dagger c_{j\uparrow} \mathcal{U} = (-1)^j c_{j\uparrow}^\dagger$, $\mathcal{U}^\dagger c_{j\downarrow} \mathcal{U} = c_{j\downarrow}$ so that the kinetic energy part in Eq. (2) stays invariant while $U \rightarrow -U$. For the operators we find $d_j \rightarrow n_{j\downarrow} - d_j$, and $m_j \rightarrow (-1)^j (1 - n_j)/2$ while $\mathcal{U}^\dagger |\Psi_D\rangle = |\Psi_N\rangle$, $\mathcal{U}^\dagger |\Psi_N\rangle = |\Psi_D\rangle$, assuming an even number of lattice sites L . (b) On a bipartite lattice, $A \otimes B$, we can furthermore apply the transformation $c_{j\sigma} \rightarrow \pm c_{j\sigma}$ for $j \in A$ ($j \in B$), respectively. This leads to $H_{-U} \rightarrow -H_U$. (c) Finally, we can use the time reversal invariance of the expectation value. Using these three symmetries we find $d_U^D(t) = 1/2 - d_U^N(t)$, $d_U^D(t) = d_{-U}^D(t)$, and $m_U^N(t) = m_{-U}^N(t)$ where $o_U^I(t) = \sum_{j=1}^L \langle o_j \rangle_U^I(t)/L$ (see Eq. (1)). We also note that $m_U^N(t) = -w_U^D(t)/2$ where $w_j = (-1)^j n_j$. The decay of $m_U^N(t)$ can therefore also be measured by the charge imbalance between even and odd sites which might be easier experimentally.

To test the LCRG algorithm, we first study the free spinful fermion (SFF) case $U = 0$ where $d_{U=0}^D(t) = (1 + J_0^2(4Jt))/4$ and $m_{U=0}^N(t) = J_0(4Jt)/2$ with J_0 being the Bessel function of the first kind. In the free SFF case, the dynamics of electrons with spin up and spin down is completely decoupled. Therefore, we can also use free spinless fermions (SLF) to calculate $m_0^N(t)$ which requires $\sqrt{\chi}$ states only to simulate the dynamics with the same accuracy. In Fig. 2(a) the LCRG results for $m_0^N(t)$ for free SFF and SLF are compared to the exact result. For free SLF with $\chi = 20000$ we can resolve 6.5 oscillations compared to the 5 oscillations which have been resolved in [16] by iTEBD. The maximum simulation time t_{max} and the accuracy of the results are, however, comparable if the same number of states are kept. We emphasize that for the Hubbard model ($M = 4$) with the conservation laws for spin and charge implemented and $\chi = 2000$ states kept, each time step takes only ~ 30 seconds on a standard PC without parallelization, which is $260\times$ faster and uses $12\times$ less memory than without conservation laws. In Fig. 2(b) the results for $d_0^D(t)$ are

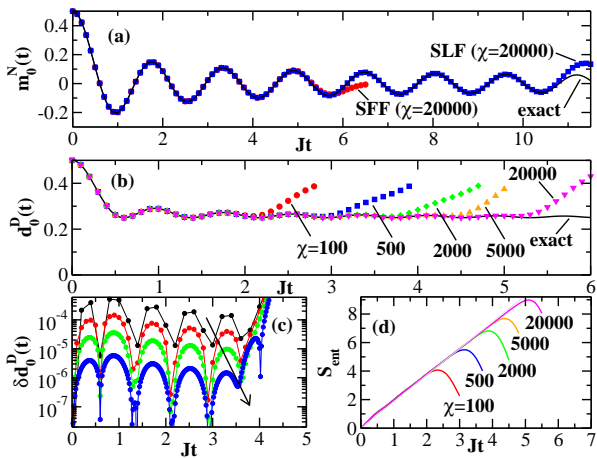


FIG. 2: (Color online) (a) $m_0^N(t)$ for free SFF (circles) and for free SLF (squares)—note that the time scale in [16] is stretched by a factor 2. (b) $d_0^D(t)$ for free SFF with χ as indicated. In both cases $\delta t = 0.1$ and lines denote the exact results. (c) Absolute error $\delta d_0^D(t)$ for free SFF with $\chi = 5000$ and $\delta t = 0.2, 0.1, 0.05, 0.02$ (in arrow direction). (d) $S_{\text{ent}}(t)$ for free SFF with $\delta t = 0.1$ and χ as indicated.

shown where χ is varied. The error of the simulation up to t_{max} is completely dominated by the error of the TSD (see Fig. 2(c)) and is of order $(\delta t)^2$ for the second order decomposition used here. Importantly, t_{max} is determined only by χ and results with in principle arbitrary accuracy can be obtained by reducing the time step δt .

The algorithm breaks down when the spectrum of the reduced density matrix ρ_s becomes dense. A suitable measure is the entanglement entropy (EE) $S_{\text{ent}}(t) = -\text{Tr} \rho_s \ln \rho_s \leq \ln(M\chi)$ with $M\chi = \dim \rho_s$. The EE is shown in Fig. 2(d) and increases linearly with time. It can be shown under very general conditions that the linear increase of the EE is a fundamental property [9] which cannot be easily overcome. The LCRG algorithm provides an intuitive picture for this behavior: The EE is proportional to the number of bonds connecting the upper and lower light cones which increases linearly with time. A breakdown of the simulation is observable as a deviation from the linear behavior and occurs when the EE is close to the bound, $S_{\text{ent}}(t) \sim \ln(M\chi)$.

Next, we study $d_V^D(t)$ in the interacting case, a situation which can be realized in ultracold gases [2]. For times $Jt \ll \min\{J/|U|, 1\}$ the relaxation is independent of the interaction strength and follows the free fermion result $d_0^D(t) \sim 1/2 - 2(Jt)^2$, see Fig. 3(a). In units of the hopping amplitude J we can simulate longer times the larger U is. This is a consequence of the slower increase of $S_{\text{ent}}(t)$ as shown in Fig. 3(b). For large U we find that the slope of the EE is given by $a \sim J/|U|$, i.e., $t_{\text{max}} \sim |U|/J^2$ and therefore set by the inverse of the magnetic superexchange interaction.

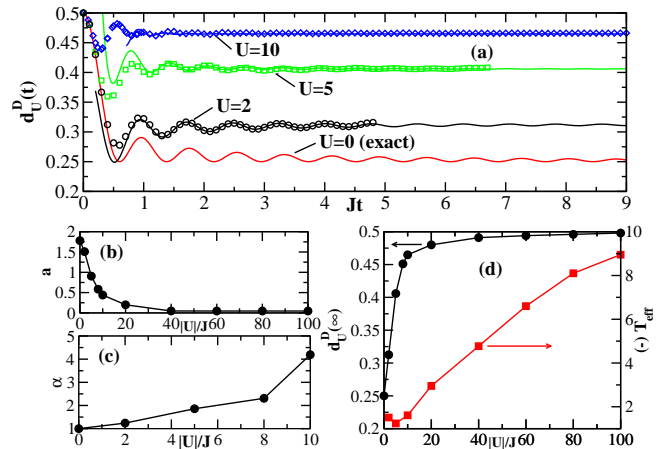


FIG. 3: (Color online) (a) $d_V^D(t)$ with $\chi = 10000$, $\delta t = 0.1$ (symbols), and fits (lines), see text. (b) Slope of the EE, $S_{\text{ent}} \sim aJt$. (c) Fitted exponent α of the power-law decay. (d) Extrapolated value $d_V^D(t \rightarrow \infty)$ and effective temperature.

At times $Jt \gg 1$ the relaxation in the free SFF case is given by $d_0^D(t) = (1 + J_0^2(4Jt))/4 \sim [1 + (4\pi t)^{-1}(1 + \cos(8Jt - \pi/2))]/4$ motivating us to fit the time dependence at finite U by $d_V^D(t) = d_V^D(\infty) + e^{-\gamma t}[A + B \cos(\Omega t - \phi)]/t^\alpha$. Such fits are shown as solid lines in Fig. 3(a). In all cases $\gamma < 10^{-3}$, i.e., we do not find evidence for a finite relaxation rate γ [21]. A relaxation following a power law has also been observed at intermediate times in a 1D Bose-Hubbard model starting from an IS with one boson on every second site [17]. On the other hand, the relaxation for the XXZ model when starting from a Néel state has been interpreted in terms of an exponential decay [16]. Our fits point to a pure power-law decay with an exponent α which increases with increasing $|U|$, see Fig. 3(c). The asymptotic value $d_V^D(\infty)$ also increases and reaches $1/2$ in the limit $|U| \rightarrow \infty$, see Fig. 3(d). We emphasize that $d_V^D(t) = d_{-U}^D(t)$, i.e., repulsive interactions lead to a binding of doublons the same way as attractive interactions do [18]. For doublons moving on a 3D lattice it has been argued that for $U > 0$ much larger than the bandwidth, many-body scattering processes are needed to dissipate the doublon energy leading to an exponentially small relaxation rate $\gamma \sim \exp(-U/J)$ [2, 14]. In our simulations we do not see any indications for a corresponding crossover time scale $\sim 1/\gamma$ at which exponential relaxation might set in. The power law decay in the Hubbard model (or, at least, the very small relaxation rate) might be a consequence of the infinitely many local conservation laws leading to integrability.

It has been suggested that observables in integrable quantum systems relax to values given by a generalized Gibbs ensemble which includes additional conservation laws [8]. However, it is not clear why only local conserved quantities specific for integrable systems and not the in-

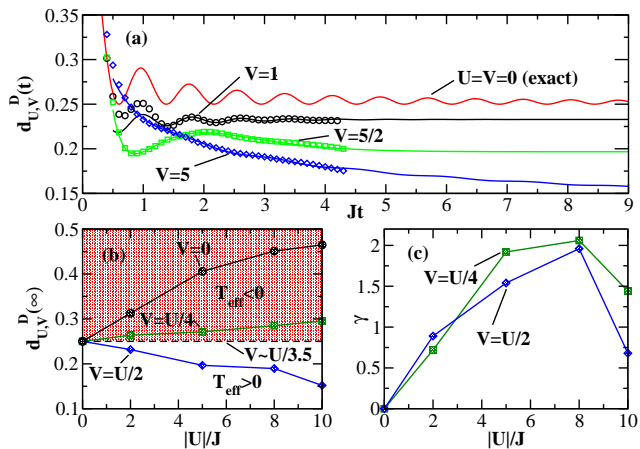


FIG. 4: (Color online) (a) $d_{U,V}^D(t)$ for $V = U/2$ with $\chi = 10000$, $\delta t = 0.1$ (symbols), and fits (lines). (b) Extrapolated values $d_{U,V}^D(t \rightarrow \infty)$. The shaded region denotes where T_{eff} is negative in the repulsive case. (c) Relaxation rate γ extracted from the fits.

finitely many non-local conserved quantities which exist for any quantum system have to be considered. Furthermore, such ensembles are impracticable in the thermodynamic limit except for the simplest free particle models [8]. Here we assign instead a temperature T_{eff} to our system in the usual canonical ensemble by demanding that $\langle d \rangle_{U,T_{\text{eff}}} = d_{U,V}^D(\infty)$ where $\langle d \rangle_{U,T} = \langle d \rangle_{-U,-T}$ denotes the thermal expectation value. Since the spectrum of our model is bounded, the use of negative temperatures is natural with $1/T \rightarrow 0^\pm$ corresponding to the case of maximum entropy. The duality transformation implies $\langle d \rangle_{U,T} + \langle d \rangle_{-U,T} = 1/2$ for all T . In particular, $\langle d \rangle_{U>0,T>0} < 1/4$ and $\langle d \rangle_{U<0,T>0} > 1/4$ with both being equal to $1/4$ in the limit $T \rightarrow \infty$. We calculate the $\langle d \rangle_{U,T}$ using the transfer-matrix DMRG [12, 19] and find that T_{eff} is negative (positive) for the repulsive (attractive) model, respectively, and $|T_{\text{eff}}|$ increases monotonically (see Fig. 3(d)) for large $|U|/J$.

Finally, we consider the non-integrable *extended Hubbard model* obtained by adding the term $H_V = V \sum_j n_j n_{j+1}$ to Eq. (2). The duality relations used for the Hubbard model are then no longer valid ($V \sum_j n_j n_{j+1} \rightarrow 4V \sum_j S_j^z S_{j+1}^z$), however, $d_{U,V}^D(t) = d_{-U,-V}^D(t)$ and $\langle d \rangle_{U,V,T} = \langle d \rangle_{-U,-V,-T}$ since these relations rely only on the lattice being bipartite and time reversal symmetry. We focus in the following on $V \leq U/2$ corresponding to a spin-density wave state in the ground state phase diagram [19]. For the case $V = U/2$ we find a qualitatively different behavior than in the Hubbard model (see Fig. 4(a)). Here $d_{U,V}^D(\infty)$ decreases with increasing interaction strength. In general, $d_{U,V}^D(\infty)$ can increase or decrease with increasing interaction strength depending on the ratio V/U . For $V \sim U/3.5$ we find

$d_{U,V}^D(\infty) \approx 1/4$ (see Fig. 4(b)) corresponding to a thermal average in the canonical ensemble with $T_{\text{eff}} = \pm\infty$. In the repulsive case we find $T_{\text{eff}} < 0$ for $V \lesssim U/3.5$ and $T_{\text{eff}} > 0$ for $V \gtrsim U/3.5$. T_{eff} changes sign as before we now do find a finite relaxation rate γ as shown in Fig. 4(c). In this case two different relaxation processes—a fast one at short time scales leading to a pre-thermalized state and a slower one setting in at $Jt \gg \exp(U/J)$ [2, 14]—could possibly exist. This might explain the non-monotonic behavior of $\gamma(U, V/U = \text{const})$ obtained when fitting with a single relaxation rate.

As an outlook we want to emphasize that contrary to iTEBD the LCRG algorithm yields results in the thermodynamic limit without requiring translational invariance. Future applications to impurity problems, disorder, and to systems with trapping potentials are therefore feasible.

The authors thank P. Barmettler and A. Rosch for valuable discussions. J.S. acknowledges support by the graduate school of excellence MAINZ/MATCOR.

-
- [1] T. Kinoshita *et al.*, Nature **440**, 900 (2006); S. Hofferberth *et al.*, Nature **449**, 324 (2007); T. Gericke *et al.*, Nat. Phys. **4**, 949 (2008); P. Würtz *et al.*, Phys. Rev. Lett. **103**, 080404 (2009); R. Sensarma *et al.*, Phys. Rev. B **82**, 224302 (2010).
 - [2] N. Strohmaier *et al.*, Phys. Rev. Lett. **104**, 080401 (2010).
 - [3] A. E. Feiguin and S. R. White, Phys. Rev. B **72**, 220401(R) (2005); A. J. Daley *et al.*, J. Stat. Mech. P04005 (2004).
 - [4] J. Sirker and A. Klümper, Phys. Rev. B **71**, 241101(R) (2005); J. Sirker *et al.*, Phys. Rev. Lett. **103**, 216602 (2009); Phys. Rev. B **83**, 035115 (2011).
 - [5] G. Vidal, Phys. Rev. Lett. **91**, 147902 (2003).
 - [6] G. Vidal, Phys. Rev. Lett. **98**, 070201 (2007).
 - [7] J. M. Deutsch, Phys. Rev. A **43**, 2046 (1991); M. Srednicki, Phys. Rev. E **50**, 888 (1994).
 - [8] A. C. Cassidy *et al.*, Phys. Rev. Lett. **106**, 140405 (2011).
 - [9] E. H. Lieb and D. W. Robinson, Commun. Math. Phys. **28**, 251 (1972); S. Bravyi *et al.*, Phys. Rev. Lett. **97**, 050401 (2006).
 - [10] S. R. White, Phys. Rev. Lett. **69**, 2863 (1992).
 - [11] A. Kemper *et al.*, J. Phys. A **36**, 29 (2003).
 - [12] R. Bursill *et al.*, J. Phys: Cond. Mat. **7**, 8605 (1995); X. Wang and T. Xiang, Phys. Rev. B **56**, 5061 (1997).
 - [13] A. Kemper *et al.*, J. Phys. A **34**, L279 (2001); T. Enss and U. Schollwöck, J. Phys. A **34**, 7769 (2001); T. Enss *et al.*, J. Phys. A: Math. Gen. **37**, 10479 (2004).
 - [14] A. Rosch *et al.*, Phys. Rev. Lett. **101**, 265301 (2008).
 - [15] R. J. Baxter, *Exactly Solved Models in Statistical Mechanics* (Academic Press, London, 1982); T. Nishino and K. Okunishi, J. Phys. Soc. Jpn. **65**, 891 (1996).
 - [16] P. Barmettler *et al.*, Phys. Rev. Lett. **102**, 130603 (2009).
 - [17] M. Cramer *et al.*, Phys. Rev. Lett. **101**, 063001 (2008).
 - [18] K. Winkler *et al.*, Nature **441**, 853 (2006).
 - [19] M. Nakamura, Phys. Rev. B **61**, 16377 (2000); S. Glocke *et al.*, Phys. Rev. B **76**, 155121 (2007).

[20] In contrast to standard corner matrices [15], the left and right matrices are identity matrices owing to the light cone structure, and the block indices of the forward and backward evolution are simply traced over.

[21] We note that the fits for large $|U|$ are more ambiguous because $d_V^D(\infty)$ is reached more quickly.